# Real-Time Traffic Volatility Forecasting in Urban Arterial Networks

Theodore Tsekeris and Antony Stathopoulos

**A methodology is presented for forecasting traffic volatility in urban arterial networks with real-time traffic flow information. This methodology provides a generalization of the standard modeling approach, in which both the mean, modeled by an autoregressive moving average process, and the variance, modeled by an autoregressive conditional heteroscedastic process, are time-varying. The statistical analysis and forecasting performance of the proposed model are investigated with real-time traffic detector data from a real urban arterial network. The results indicate the potential of the proposed model to improve the accuracy of predicted traffic volatility across different lengths of forecasting horizon in comparison with the standard generalized autoregressive conditional heteroscedastic methodology.**

Forecasting of traffic conditions constitutes a valuable tool for the management and control of dynamic transportation networks. The complexity of this task increases with the frequency of data retrieval, particularly when one is dealing with traffic flow measurements obtained from loop detectors every few minutes. Several methods have been developed and applied for the short-term prediction of traffic flow, mostly on freeways and, to a smaller extent, on urban arterial networks. Examples of such methods include time series models (*1*), nonparametric regression models (*2*), dynamic traffic assignment models (*3*), Kalman filtering (*4*), neural networks (*5*), state-space methods (*6*), and chaos theory models (*7*).

A crucial aspect of the description of urban traffic flow refers to its time-dependent variation—that is, its volatility—which provides a measure of the unpredictability of traffic conditions. The fact that traffic flow variation displays time-dependent behavior has been demonstrated in several recent studies (*8*, *7*). In practice, the measurement of volatility allows for the identification of confidence bounds for the traffic forecasts. These bounds have considerable implications for the deployment of systems designed to disseminate real-time traffic information to travelers, such as the advanced traveler information system (ATIS). In addition, the determination of the boundary conditions of traffic forecasts enables the identification of congestion onset and the timely selection of appropriate traffic control actions within the context of advanced traffic management systems (ATMS).

The modeling of volatility presumes not only that traffic flow (mean) levels are conditional upon the past levels of flow but also that their variance is time variant or conditionally heteroscedastic. Specifically, the error term is assumed to be serially correlated and can be modeled by an autoregressive (AR) process. Kamarianakis et al. (*9*) recently implemented an econometric approach that combines an autoregressive integrated moving average (ARIMA) process (*10*) to model the conditional mean and a generalized autoregressive conditional heteroscedastic (GARCH) process to model the conditional variance. Their application was based on traffic flow data that originated from a real urban arterial network, the road network of Athens, Greece. Nonetheless, the proposed model was static and provided in-sample estimates rather than actual forecasts of traffic volatility. In addition, the specification of the error correlation structure in the ARIMA-GARCH model is independent from the sample observations, whereas the improvements in volatility forecasts have been found to lead to reduced forecasting performance for the traffic flow levels (*9*).

An alternative autoregressive conditional heteroscedastic (ARCH)–type methodology is presented here to address the foregoing problems and improve the accuracy of traffic volatility forecasting in urban arterial networks.

## DESCRIPTION OF MODELS

### Mean Equation

A univariate time series of traffic flow $y_t$ can be defined in its functional form through the so-called mean equation as follows:

$$y_t = E\left(y_t \middle| \Omega_{t-1}\right) + \epsilon_t \tag{1}$$

where $E(.|.)$ denotes the conditional expectation (mean) operator and refers to the predictable part of $y_t$ and $\epsilon_t$ is the disturbance term (or shock) and refers to the unpredictable part of $y_t$. The combination of the AR and the moving average (MA) models leads to the specification of the ARIMA model of order $n$ and $s$, with the following form:

$$\psi(L) y_t = \theta(L) \epsilon_t \tag{2}$$

with

$$\psi(L) = 1 - \sum_{i=1}^{n} \psi_i L^i$$

$$\theta(L) = 1 + \sum_{j=1}^{s} \theta_j L^j$$

and $L$ a lag operator such that $L^k y_t = y_{t-k}$. Several studies (*6*, *8*) have shown that traffic flows may exhibit significant autocorrelation between successive observations over time. In such a case, it can

Department of Transportation Planning and Engineering, School of Civil Engineering, National Technical University of Athens, 5 Iroon Polytechniou, 157 73 Athens, Greece.

*Transportation Research Record: Journal of the Transportation Research Board, No. 1964*, Transportation Research Board of the National Academies, Washington, D.C., 2006, pp. 146–156.

arguably be considered that $y_t$ displays long memory or long-term dependence and is best modeled by extending the aforementioned ARIMA($n$, $s$) process to an autoregressive fractionally integrated moving average (ARFIMA) process (*10*). The ARFIMA($n$, $\zeta$, $s$) process is given as follows:

$$\psi(L)(1-L)^{\zeta} y_t = \theta(L)\epsilon_t \tag{3}$$

where the operator $(1 - L)^{\zeta}$ accounts for the long memory of the process and is defined as

$$(1-L)^{\zeta} = 1-\sum_{k=1}^{\infty} c_k(\zeta) L^k \tag{4}$$

with $0 < \zeta < 1$, $c_1(\zeta) = \zeta$, $c_2(\zeta) = \frac{1}{2}\zeta(1 - \zeta)$, . . . , and the truncation order of the infinite summation is set equal to $t - 1$.

## Variance Equation

### GARCH Model

According to Engle (*11*), the ARCH process of order $q$ assumes that a shock $\epsilon_t$ has the following form:

$$\epsilon_t = z_t \sigma_t \tag{5}$$

and the conditional variance $\sigma_t^2$ is given as follows:

$$\sigma_t^2 = \omega + \sum_{i=1}^{q} \alpha_i \epsilon_{t-i}^2 \tag{6}$$

where constant $\omega > 0$ captures fixed effects, $\Sigma_i^q = 1\alpha < 1$, $\alpha_i \geq 0$ (for $i = 1, \ldots, q$), and $z_t$ is independent and identically distributed and has a probability density function $D(0,1)$ with mean 0 and unit variance (see the section on case study and experimental setup). The foregoing process describes volatility clustering by assuming that the conditional variance of $\epsilon_t$ is an increasing function of the square of the shock $\epsilon_{t-1}$ that occurred in $t - 1$. Moreover, this process can explain part of the excess kurtosis or fat tails (with values of kurtosis coefficient typically larger than 3) and the existence of skewness (which corresponds to a positive or negative skewness coefficient) in the distribution of traffic flow (see the section on case study and experimental setup).

The ARCH($q$) model typically requires a very large number of parameters to be estimated in order to capture the dynamics of the conditional variance. To overcome this shortcoming, Bollerslev (*12*) proposed the GARCH model by adding lagged conditional variances to the ARCH model. The GARCH($p$, $q$) model can be expressed as follows:

$$\sigma_t^2 = \omega + \sum_{i=1}^{q} \alpha_i \epsilon_{t-i}^2 + \sum_{j=1}^{p} \beta_j \sigma_{t-j}^2 \tag{7}$$

with the lag operator $L$, Equation 7 is reduced to

$$\sigma_t^2 = \omega + \alpha(L)\epsilon_t^2 + \beta(L)\sigma_t^2 \tag{8}$$

with $\alpha(L) = \alpha_1 L + \alpha_2 L^2 + \cdots + \alpha_q L^q$, $\beta(L) = \beta_1 L + \beta_2 L^2 + \cdots + \beta_p L^p$, $\omega > 0$, $\alpha_i \geq 0$ (for $i = 1, \ldots, q$), and $\beta_j \geq 0$ (for $j = 1, \ldots, p$). Then, assuming that all roots of the polynomial $|1 - \beta(L)| = 0$ lie outside the unit circle, one obtains

$$\sigma_t^2 = \omega[1-\beta(L)]^{-1} + \alpha(L)[1-\beta(L)]^{-1}\epsilon_t^2 \tag{9}$$

Equation 9 essentially presents the GARCH($p$, $q$) model as an ARCH($\infty$) process by making the conditional variance linearly dependent on all previous squared residuals.

### Fractionally Integrated Asymmetric Power ARCH Model

The GARCH model implies that if $\epsilon_{t-1}$ is large (small) in absolute value, $\sigma_t^2$ and hence $\epsilon_t$ are also expected to be large (small) in absolute value. This linear relationship between the conditional variance and all shocks in the past (see Equation 9) imposes a rigidity in describing volatility dynamics, since it does not allow the model to adjust itself to the existing set of information, that is, the sample observations available in each particular case. In addition, the GARCH model does not allow for the effect of asymmetries to be taken into consideration. The asymmetric effect refers to the fact that the impact of a negative shock $\epsilon_t$ may be negatively correlated with the forecast of conditional variance $\sigma_t^2$; namely, it may result in an increase of volatility and vice versa.

Several alternative model specifications have appeared in the literature during the last few years (*13*, pp. 778–878) in order to address the aforementioned problems. Among them, the asymmetric power ARCH model (*14*), referred to as the APARCH model, can offer a suitable generalization of the standard ARCH and GARCH models in order to adequately represent the effects of nonlinearity and asymmetry on the volatility forecasts. This achievement is made possible through the power transformation of the conditional variance, which relaxes the linear dependence of conditional variance on all previous squared residuals and allows for the effect of sign and magnitude of previous shocks on future volatility forecasts to be considered. The APARCH($p$, $q$) model can be expressed as follows:

$$\sigma_t^{\delta} = \omega + \sum_{i=1}^{q} \alpha_i \left(|\epsilon_{t-i}| - \gamma_i \epsilon_{t-i}\right)^{\delta} + \sum_{j=1}^{p} \beta_j \sigma_{t-j}^{\delta} \tag{10}$$

with exponent $\delta > 0$ and asymmetry coefficient $-1 < \gamma_i < 1$ (for $i = 1, \ldots, q$). When $\gamma_i > 0$ (<0), negative (positive) shocks give rise to higher volatility than positive (negative) shocks. On the basis of Equation 10, the ARCH($q$) model can be considered as an extension of the APARCH($p$, $q$) model when $\delta = 2$, $\gamma_i = 0$, and $\beta_j = 0$. Similarly, the GARCH($p$, $q$) model can be obtained from the APARCH($p$, $q$) model by setting $\delta = 2$ and $\gamma_i = 0$.

The ARCH($q$) and GARCH($p$, $q$) processes are based respectively on the assumptions that the propagation of shocks occurs at an exponential rate of decay, which captures only the short memory of the volatility dynamics, and that the persistence of shocks is infinite. In order to relax these (seemingly) restrictive assumptions, Tse (*15*) proposed the extension of the APARCH model to the fractionally integrated asymmetric power ARCH model, or FIAPARCH model. By using the lag operator $L$, the APARCH ($p$, $q$) model can be expressed as follows:

$$\sigma_t^{\delta} = \omega + \alpha(L)\left(|\epsilon_t| - \gamma\epsilon_t\right)^{\delta} + \beta(L)\sigma_t^{\delta} \tag{11}$$

Equation 11 can be rewritten as follows:

$$\left[1-\alpha(L)-\beta(L)\right]\left(|\epsilon_t|-\gamma\epsilon_t\right)^{\delta} = \omega+\left[1-\beta(L)\right]\left[\left(|\epsilon_t|-\gamma\epsilon_t\right)^{\delta}-\sigma_t^{\delta}\right] \quad (12)$$

To modify the APARCH model such that it considers the long memory or long-term dependence of the conditional variance on the effect of a shock, a polynomial $\phi(L)$ is introduced in Equation 12 as follows:

$$(1-L)^d\phi(L)\left(|\epsilon_t|-\gamma\epsilon_t\right)^{\delta} = \omega+\left[1-\beta(L)\right]\left[\left(|\epsilon_t|-\gamma\epsilon_t\right)^{\delta}-\sigma_t^{\delta}\right] \quad (13)$$

with $\phi(L) = [1 - \alpha(L) - \beta(L)](1 - L)^{-d}$ and the roots of the equation $\phi(L) = 0$ being outside the unit circle. The fractional differencing operator $(1 - L)^d$ is by construction similar to the operator $(1 - L)^{\zeta}$ of the ARFIMA model used previously for the mean equation. Specifically, it holds that

$$(1-L)^d = 1-\sum_{k=1}^{\infty}c_k(d)L^k \quad (14)$$

with $0 < d < 1$, $c_1(d) = d$, $c_2(d) = \frac{1}{2}d(1-d)$, . . . , and the truncation order of the infinite summation is set equal to $t - 1$. With the terms rearranged, Equation 13 can be written as follows:

$$\sigma_t^{\delta} = \eta+\left\{1-\left[1-\beta(L)\right]^{-1}\phi(L)(1-L)^d\right\}\left(|\epsilon_t|-\gamma\epsilon_t\right)^{\delta} \quad (15)$$

with $\eta = \omega/[1 - \beta(1)]$. The FIAPARCH($p$, $d$, $q$) model expressed by Equation 15 can incorporate the flexibility of the APARCH model (see Equation 10) while it helps fill the gap between short and infinite persistence of shock effects on future volatility by making the effects of a shock take a considerable time to decay, that is, at a slow hyperbolic rate. The application of a methodology is presented here that combines the ARFIMA($n$, $\zeta$, $s$) process to model the conditional mean with the FIAPARCH($p$, $d$, $q$) process to model the conditional variance, which is referred to here as the ARFIMA-FIAPARCH model. This model is compared with the standard ARIMA-GARCH model, which involves neither fractionally integrated components nor the power transformation and asymmetric effects in its specification, as they were described earlier.

Despite the fact that volatility models, such as those described, mostly find application in the forecasting of financial market returns, their usage in transportation networks can be justified through the intrinsic similarities between market players and network users. According to Helbing et al. (*16*), the volatile decision dynamics of transportation network users have been found to be similar to the volatility clustering of players' decisions in financial stock markets. Particularly in the context of congested arterial networks, the presence of shocks in the traffic process makes some users change their driving behavior to compensate for the resulting changes in expected travel times. These changes give rise to increased volatility, whose rate tends to decay over time in order to restore the past stability in the system. Because of congestion conditions, the effect of shocks on the changing rate of volatility may be reasonably assumed to decay slowly over time. Thus, volatile traffic behavior can arguably be predicted more accurately by using a fractionally integrated process in the variance equation through the FIAPARCH process rather than by using the standard GARCH process. In addition, the power transformation in the variance equation in the FIAPARCH process can provide a more plausible and flexible modeling of the response of traffic behavior to the presence of shocks in comparison with the exponential structure of the GARCH model.

## CASE STUDY AND EXPERIMENTAL SETUP

### Case Study Characteristics

The ARIMA-GARCH and ARFIMA-FIAPARCH models are investigated here by using actual traffic flow data collected every 90-s cycle from loop detectors located in major signalized arterial streets of a real urban network, the road network of Athens, Greece. These loop detectors correspond to Loop Detector 78 (L78), 101 (L101), 102 (L102), and 108 (L108). All four detectors are situated along an important three-lane-per-direction urban corridor on the periphery of the core area of the city (Alexandras Avenue). Detector L78 is located upstream of L102, along the direction from the downtown to the periphery of the city. Detector L101 is located downstream of L108, along the direction from the periphery to the core area of the city. The total time period of the sample was in May 2000. Because of the fact that flows vary significantly between weekdays and weekends, data from Saturdays and Sundays were excluded from the given sample, yielding a data set that consists of flow (volume) and occupancy measurements for 22 days and contains 10,560 three-minute observations. The data aggregation frequency of 3 min can provide a sufficiently short observation period so that it retains important information about the true state of traffic volatility.

The variable used here to describe the dynamics of traffic flow and its volatility is relative velocity as it is defined by the ratio of volume to occupancy. This metric is a factored expression of traffic flow (expressed in vehicles per unit of time) multiplied by the inverse of the loading fraction of the roadway. The expression provides a proxy for the average space-mean speed since it takes into account the flow rate conditions under which it takes place. This measure can provide a clearer representation of time-varying changes in the traffic regime and lead to more accurate traffic forecasts (*6, 9*). Furthermore, the first-order difference ($\Delta$) of the relative velocity values corresponding to any two successive observation periods of each day was used to provide the increments or decrements of relative velocities. The differencing process eliminates the underlying impact of diurnal periodic trends (periodicities) on the forecasts of volatility dynamics.

The given set of traffic flow information has been found to exhibit significant nonlinearity and nonstationarity on the basis of appropriate statistical tests undertaken in other studies for the same signalized arterials and data set (*6, 17*). In addition, the nonstationarity of the traffic conditions in the given area, in terms of the relative velocity, was preliminarily investigated in the current study on the basis of the ARCH statistical test of Engle (*11*), and it was found to be statistically significant for all loop measurement locations at the 99% confidence level (see also section Results and Analysis). Table 1 summarizes

**TABLE 1 Descriptive Statistics of Difference of Relative Velocities in Each of Four Loop Measurement Locations**

| Loop | Mean | Variance | Skewness | Kurtosis |
|---|---|---|---|---|
| L78 | –0.00002 | 0.11225 | –0.23650 | 7.53697 |
| L101 | 0.00093 | 0.72752 | –0.19322 | 9.69141 |
| L102 | –0.00043 | 0.37563 | 0.09726 | 3.72945 |
| L108 | –0.00024 | 0.98698 | 0.54603 | 17.467 |

the basic statistical measures of the Δ of relative velocities in each of the four locations used in the study. The results indicate the considerably different (positive or negative) skewness and kurtosis of the relative velocities among the various locations of the study. In particular, the values of the kurtosis coefficient signify the excess kurtosis, that is, the existence of fat tails in the distribution of relative velocity within the given sample period.

The divergent magnitude of the variance corresponding to each of the four time series denotes the important differences in the state of traffic volatility between the various loop measurement locations. Moreover, Figure 1 illustrates the diurnal dynamics of the relative velocity in each of the four loop measurement locations during a typical weekday, the first day of the forecast, as discussed later. These graphs verify the significantly different dynamics pertaining to the

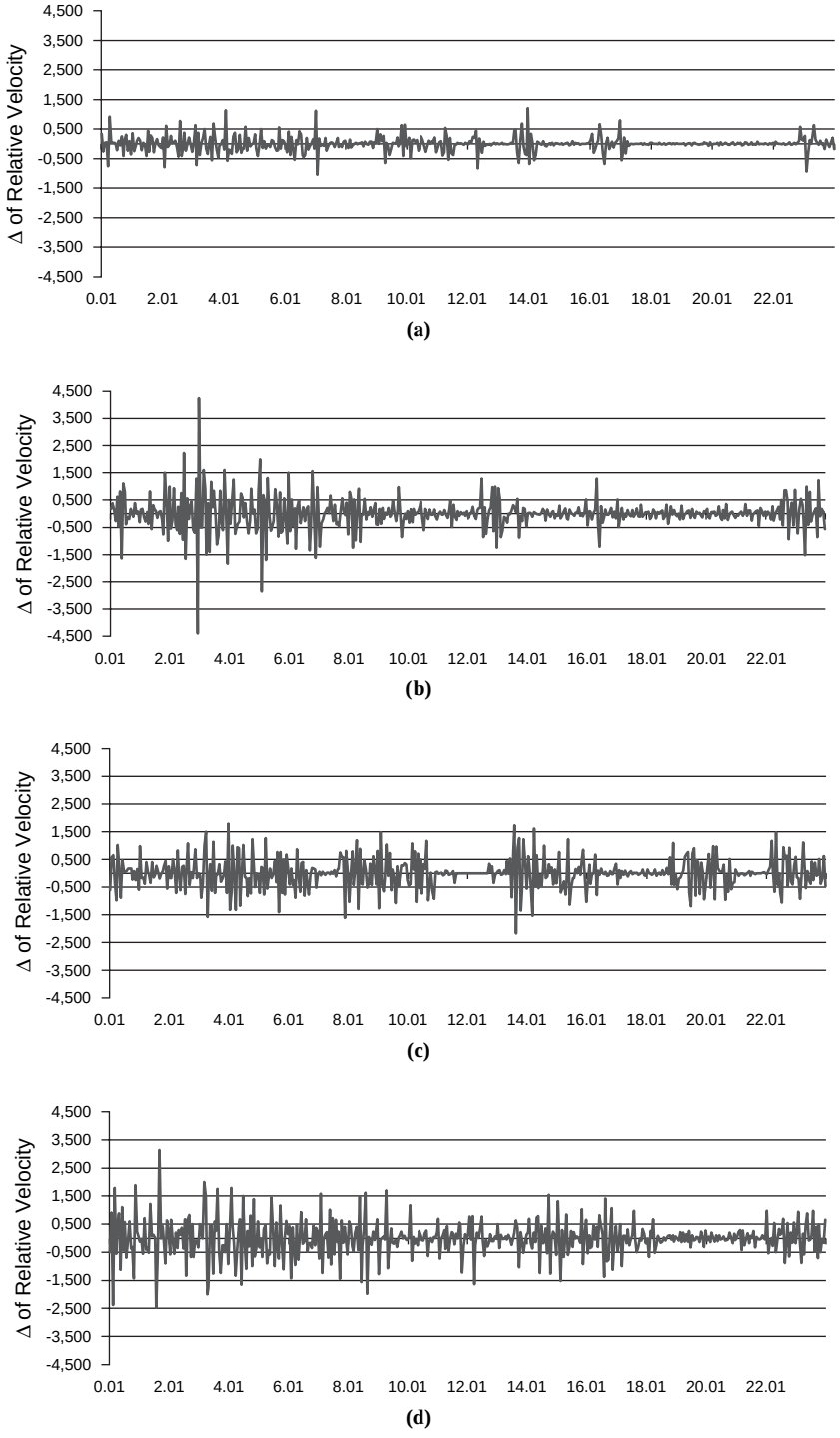


FIGURE 1 Diurnal dynamics of relative velocity during typical weekday for loop measurement locations (*a*) L78, (*b*) L101, (*c*) L102, and (*d*) L108.

traffic volatility between different periods of the day as well as different locations in the urban corridor under study.

### Experimental Setup

The primary purpose of this study is the short-term forecasting of traffic volatility. For this reason, a holdout subsample with a size equal to 10% of the total sample size, which approximately corresponds to the last 2 weekdays of the whole sample period, is employed here to evaluate the actual forecasting performance of the models in real-time traffic conditions in comparison with the approach of in-sample forecasting. Then the models are used for the estimation of the conditional expectation $\tilde{y}_{t+h|t}$, which is the optimal $h$-step-ahead prediction of $y_{t+h}$ given the information obtained until time $t$, where $h$ is the step of forecasting. The models also provide estimates of the future volatility $\tilde{\sigma}^2_{t+h|t}$, which is the optimal $h$-step-ahead prediction of conditional variance $\sigma^2_{t+h}$ given the information obtained until time $t$. In order to evaluate the effect of increasing the length of the forecasting horizon on the model performance, three different prediction steps are used here. These prediction steps refer to $h = 1$ (one step ahead) corresponding to a forecasting period of 3-min length, $h = 5$ corresponding to a forecasting period of 15-min length, and $h = 10$ corresponding to a forecasting period of 30-min length.

The calculation of $\tilde{y}_{t+h|t}$ and $\sigma^2_{t+h|t}$ is carried out recursively, through solution of the ARIMA-GARCH and ARFIMA-FIAPARCH models based on the quasi maximum likelihood estimation (QMLE) method as provided by the *G@RCH* software (*18*) written in the *Ox* matrix programming language (*19*). This software offers a unique library for the building, solution, and testing of ARCH-type models, with at least the same desirable features as other existing statistical software dealing with such types of models. In addition, a normal (Gaussian) distribution is assumed here for the probability density function $D(.)$ of the $z_t$-process in Equation 5 because the adoption of other, more realistic statistical distributions capable of explicitly representing the effects of skewness and kurtosis, such as the skewed Student's $t$-distribution, as provided through the *G@RCH* software, was not found to result in an improvement in the forecasting performance of the models. This outcome can be possibly attributed to the relatively short temporal lengths of the forecasting horizons used in this study (as discussed earlier) in comparison with longer forecasting horizons, such as those of one day, one week, and so on, in which the effect of skewness and kurtosis can have a larger impact on long-term volatility forecasts. Both models demonstrated the ability to converge within a reasonable computing time (<2 min with a Pentium III processor with 128 MB of RAM), which permits their implementation in real-time traffic conditions, with the ARFIMA-FIAPARCH model to involve the heaviest computational burden.

## RESULTS AND ANALYSIS

### Statistical Analysis of Models

Table 2 presents the (best-fit) estimated ARIMA-GARCH and ARFIMA-FIAPARCH models, including the statistical significance of the model coefficients based on the Student's $t$-test statistic. Furthermore, in order to examine the stability of the model parameters, the two models were reestimated by using half the number of observations. As is common in many applications of the ARCH-type models (*13*), including those in transportation networks (*9*), FIAPARCH(1, $d$, 1) as well as GARCH(1, 1) specification was found to result in the most adequate representation of the volatility dynamics through the use of appropriate information criteria (*18*). Similarly, an ARFIMA(1, $\zeta$, 1) as well as an ARIMA(1, 1) specification were adopted in order to ensure ease in development and application of the two models and facilitate the comparison between them.

Both the AR ($\psi$) and the MA ($\theta$) coefficients (see Equation 2), referred to as AR(1) and MA(1) in Table 2, were generally found to be statistically significant in modeling the conditional expectation over different locations and information sets. Correspondingly, the ARCH ($\alpha$) and the GARCH ($\beta$) coefficients (see Equation 8), referred to as ARCH(1) and GARCH(1) in Table 2, were generally found to be statistically significant in modeling the conditional variance of the models. The constant terms of the conditional mean and the conditional variance of the two models are not included in Table 2 since their effect was generally found to be statistically nonsignificant for the cases considered in the current study.

The long-memory parameter (exponent $d$) in the FIAPARCH model (Equation 15), referred to as FDIF(V) in Table 2, was found to be statistically significant and statistically significantly different from zero and unity ($0.2 < d < 0.8$ for all cases considered). This result gives support to the modeling of fractionally integrated conditional heteroscedasticity and rejects the hypotheses of short-run and infinite persistence of shock effects on volatility dynamics. In contrast, the long-memory parameter (exponent $\zeta$) in the ARFIMA model (Equation 3), referred to as FDIF(M) in Table 2, was found to be statistically significant only for the case of L108. In the remaining three locations, the $\zeta$-parameter was found to be statistically nonsignificant, with $d < 0.2$. These results indicate that the existence of long-term dependence in the conditional mean is not so evident as in the conditional variance. This long-term dependence may be suppressed by the quality of traffic signal coordination or other congestion phenomena affecting the traffic conditions in the particular area (*6*).

Furthermore, the asymmetry parameter ($\gamma$) in the FIAPARCH model, referred to as ASMTRY in Table 2, was not found to be statistically significant in any of the cases considered ($|\gamma| < 0.5$). This result leads to the rejection of the hypothesis that negative (positive) shocks give rise to higher volatility than positive (negative) shocks. On the contrary, the exponent coefficient $\delta$ in the FIAPARCH model, referred to as EXPNT in Table 2, was found to be statistically significant in all cases considered, with $\delta > 1.0$. This outcome allows the FIAPARCH model to adapt a more flexible form to express the relationship between the conditional variance and the shocks that occurred in the past, on the basis of the existing sample observations. In addition, Table 2 shows that the statistical significance of the model coefficients for the two cases using the whole set and the half-set of observations does not practically change. This fact provides evidence of the parametric stability of the two models, since it is also confirmed by the joint tests based on the likelihood ratio statistic (*18*).

### Comparison of Forecasting Performance

The main purpose of developing the ARIMA-GARCH and ARFIMA-FIAPARCH models in this study is to produce short-term predictions of the time-dependent changes in the mean and the variance of traffic flow, as expressed by the relative velocity. Despite the fact that the long-memory parameter $\zeta$ of the ARFIMA process was found to be statistically nonsignificant, except in the case of the L108 detector, the fractional differencing operator is retained in the specification of the mean equation; that is, the ARFIMA-FIAPARCH model is also

**TABLE 2 Estimated ARIMA-GARCH and ARFIMA-FIAPARCH Models**

| Loop | Model \ Parameter | AR(1) | MA(1) | ARCH(1) | GARCH(1) | FDIF(M) | FDIF(V) | ASMTRY | EXPNT |
|---|---|---|---|---|---|---|---|---|---|
| L78 | ARIMA-GARCH | 0.423 | –0.854 | 0.173 | 0.772 | | | | |
| | (*t*-stat) | 8.926 | –32.67 | 3.691 | 13.794 | | | | |
| | | (0.442) | (–0.877) | (0.206) | (0.54) | | | | |
| | (*t*-stat) | (6.48) | (–22.1) | (2.113) | (10.217) | | | | |
| | ARFIMA-FIAPARCH | 0.35 | –0.886 | 0.253 | 0.548 | 0.137 | 0.508 | –0.211 | 1.558 |
| | (*t*-stat) | 6.523 | –20.008 | 2.004 | 4.85 | 1.779 | 2.908 | –1.58 | 4.833 |
| | | (0.263) | (–0.598) | (0.463) | (0.694) | (0.104) | (0.427) | (0.349) | (1.542) |
| | (*t*-stat) | (2.083) | (–7.407) | (1.856) | (7.409) | (1.425) | (2.755) | (1.842) | (3.081) |
| L101 | ARIMA-GARCH | 0.257 | –0.806 | 0.08 | 0.895 | | | | |
| | (*t*-stat) | 4.709 | –26.87 | 2.18 | 30.155 | | | | |
| | | (0.233) | (–0.819) | (0.046) | (0.927) | | | | |
| | (*t*-stat) | (3.224) | (–19.54) | (2.07) | (25.72) | | | | |
| | ARFIMA-FIAPARCH | 0.343 | –0.709 | 0.368 | 0.760 | –0.181 | 0.523 | –0.14 | 1.845 |
| | (*t*-stat) | 2.726 | -4.36 | 2.13 | 7.374 | –1.723 | 3.039 | –0.591 | 5.842 |
| | | (0.223) | (–0.834) | (0.235) | (0.728) | (–0.086) | (0.395) | (–0.428) | (1.386) |
| | (*t*-stat) | (2.019) | (–6.658) | (1.503) | (11.24) | (–0.693) | (2.752) | (–1.453) | (3.264) |
| L102 | ARIMA-GARCH | 0.281 | –0.795 | 0.138 | 0.795 | | | | |
| | (*t*-stat) | 4.254 | –18.39 | 3.595 | 18.6 | | | | |
| | | (0.184) | (–0.81) | (0.171) | (0.714) | | | | |
| | (*t*-stat) | (2.492) | (–19.37) | (3.676) | (13.527) | | | | |
| | ARFIMA-FIAPARCH | 0.261 | –0.581 | –0.59 | –0.812 | –0.171 | 0.309 | 0.15 | 1.280 |
| | (*t*-stat) | 2.385 | –13.589 | –4.154 | –7.606 | –1.493 | 2.644 | 0.202 | 4.519 |
| | | (0.219) | (–0.617) | (–0.38) | (–0.696) | (–0.198) | (0.286) | (0.192) | (1.079) |
| | (*t*-stat) | (3.136) | (–15.931) | (–2.464) | (–4.844) | (–1.813) | (2.273) | (0.594) | (3.203) |
| L108 | ARIMA-GARCH | 0.124 | –0.825 | 0.109 | 0.861 | | | | |
| | (*t*-stat) | 2.518 | –42.34 | 4.299 | 31.80 | | | | |
| | | (0.081) | (–0.817) | (0.127) | (0.846) | | | | |
| | (*t*-stat) | (1.878) | (–25.22) | (3.213) | (22.92) | | | | |
| | ARFIMA-FIAPARCH | 0.267 | –0.006 | 0.299 | 0.77 | 0.238 | 0.634 | –0.095 | 2.149 |
| | (*t*-stat) | 3.719 | –50.67 | 2.603 | 9.881 | 3.092 | 3.525 | –1.038 | 9.377 |
| | | (0.218) | (–0.091) | (0.185) | (0.871) | (0.206) | (0.751) | (–0.038) | (2.416) |
| | (*t*-stat) | (2.691) | (–30.26) | (2.022) | (10.53) | (2.57) | (3.368) | (–0.43) | (6.964) |

NOTE: Values in parentheses correspond to results obtained using 50% of the observations.

used in the forecasting part of the study instead of the corresponding ARIMA-FIAPARCH model. This model is used because the existence of a fractional differencing operator in both the mean and the variance equations has been shown to prevent the problem of structural differences in the parameterization of the two equations. This parallelism in the parametric structure of the two equations has proved to retain a balance between the forecasting performance of the conditional mean and the conditional variance (*20*).

More specifically, on the one hand, the adoption of the FIAPARCH specification for the variance equation improves the accuracy of the volatility forecasts in comparison with the adoption of the standard GARCH specification. On the other hand, the adoption of the ARFIMA instead of the standard ARIMA specification for the mean equation enables such an improvement without sacrificing accuracy in the forecasts of the traffic flow levels (as discussed also later). The superior forecasting performance of the ARFIMA-FIAPARCH model in comparison with that of the ARIMA-FIAPARCH model was observed through several test experiments conducted with the current data set in the given area, and it has been theoretically proved in the literature as well for other application domains (*20*).

Figure 2 shows the real-time forecasts of traffic volatility with the proposed model, that is, the ARFIMA-FIAPARCH model, across the first weekday of the forecasting period (see section Case Study and Experimental Setup) by using a set of different prediction steps, $h = 1$, $h = 5$, and $h = 10$. The sequential succession of tranquil and volatile periods denotes that the predicted volatility displays significant intraday dynamics as well as spatial differences across the particular corridor under study. These trends are consistent with the diurnal changing dynamics of the (observed) relative velocity at each of the four loop measurement locations during the same weekday, as shown in Figure 1. By comparing the three graphs corresponding to the three different prediction steps, one can observe that the level of volatility clearly diminishes with the length of the forecasting horizon. This finding agrees with the results of similar studies conducted in other application fields (*13*). More specifically, the increase of the length of the forecasting horizon and of the amount of traffic

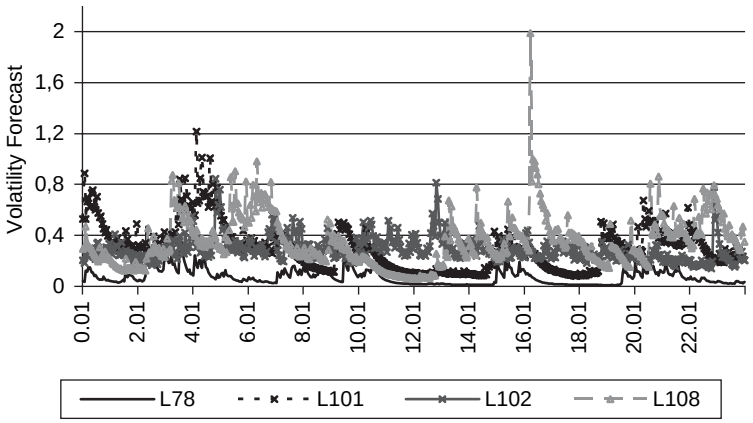


**(a)**

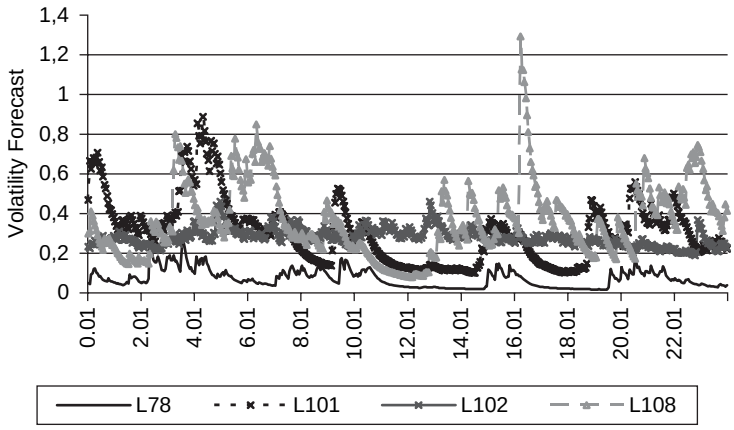


**(b)**

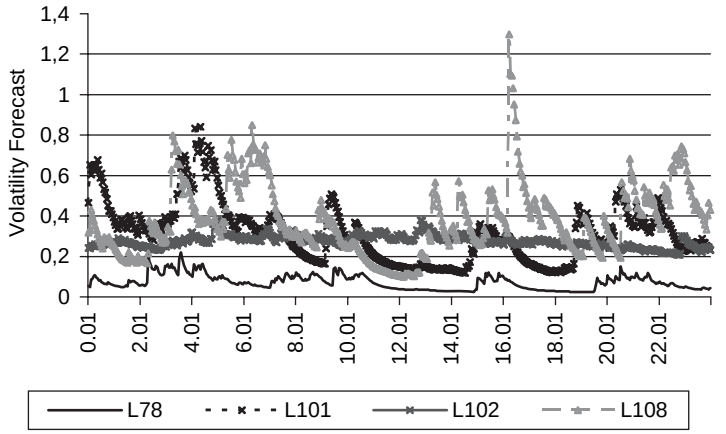


**(c)**

**FIGURE 2 Real-time forecasts of traffic volatility across first weekday of forecasting period with prediction steps (*a*) $h = 1$, (*b*) $h = 5$, and (*c*) $h = 10$.**

information processed leads to more smoothed values of future volatility because a jagged time-series graph of short-time measurements would smooth over longer period measurements, since those measurements reflect averaged fluctuations of traffic.

Figures 3, 4, and 5 provide a comparison of the forecasting performance of the ARIMA-GARCH and ARFIMA-FIAPARCH models by using, respectively, prediction steps $h = 1$, $h = 5$, and $h = 10$. The forecasting performance of the two models is evaluated here by using the standard measure of the mean absolute error (MAE) between the predicted and the actual (realized) values of the conditional variance as well as the conditional mean, denoted here as MAE(V) and MAE(M), respectively. Both measures generally appear to grow with

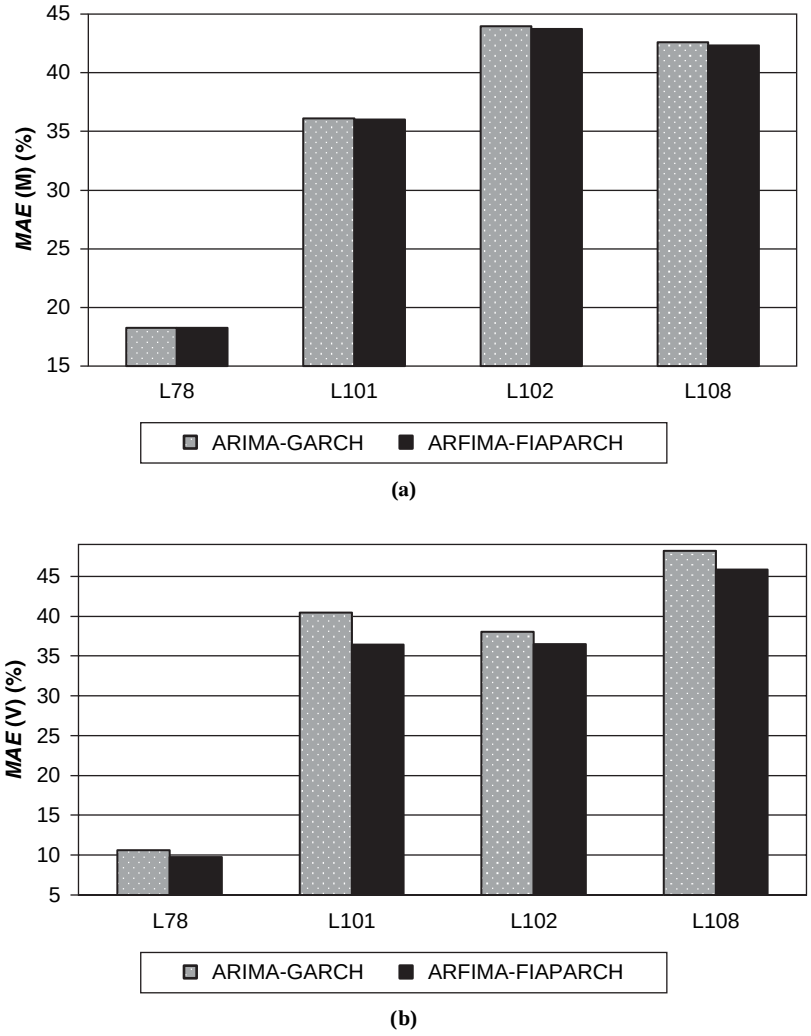


FIGURE 3 Comparison of forecasting performance of ARIMA-GARCH and ARFIMA-FIAPARCH models in terms of (*a*) MAE(M) and (*b*) MAE(V) with Prediction Step $h = 1$.

the increase in the size of the prediction step. This fact can be attributed to the added uncertainty associated with the future traffic levels and volatility state as the length of the forecasting horizon increases.

The results shown in Figures 3 to 5 provide evidence of the superior performance of the ARFIMA-FIAPARCH model in comparison with the ARIMA-GARCH model in forecasting traffic volatility in terms of producing lower MAE(V) values for all loop measurement locations and prediction steps. The ARFIMA-FIAPARCH model attains these accuracy gains in volatility forecasts without degrading the forecasting accuracy of the traffic flow levels in relation to the ARIMA-GARCH model, since the MAE(M) values are basically the same for both models in all the cases considered. The differences between the values of the MAE(M) and MAE(V) corresponding to different locations can be attributed to the varying levels of volatility pertaining to each of these locations. In particular, the significantly lower values of the MAE(M) and MAE(V) corresponding to L78 can be explained by the considerably less volatile (more tranquil) traffic conditions prevailing in the specific location in comparison with the conditions prevailing in the other locations (see Figure 1).

The values of the MAE(M) appear rather high, particularly for locations L101, L102, and L108, when compared with values reported in freeway traffic studies. This fact can be possibly attributed to the data available and the present urban network characteristics rather than to the methodology used. That is, the measured level of accuracy verifies that traffic flow in signalized urban arterials cannot be predicted, at least in the short run, with as much accuracy as flow in urban freeways. Nonetheless, the results of the study signify the relative benefits and potential usefulness of developing new forecasting methodologies, such as that of the ARFIMA-FIAPARCH model, to predict traffic volatility more accurately on the basis of the MAE(V) in urban arterial networks in comparison with the use of existing forecasting methodologies.

Moreover, the results clearly show that larger gains in the accuracy of the predicted volatility can be achieved for the ARFIMA-FIAPARCH model in comparison with the ARIMA-GARCH model when longer forecasting horizons, such as 15 and 30 min, are adopted. More specifically, the smallest improvements range from 4.0% (for $h = 1$) to 5.2% (for $h = 10$) in the case of L102, whereas the largest improvements range from 10.0% (for $h = 1$) to 14.4% (for $h = 10$) in the case of L101. These differences in the accuracy gains of volatility forecasts can be attributed to the ability of the ARFIMA-FIAPARCH model to allow for correlations of the conditional variance with the

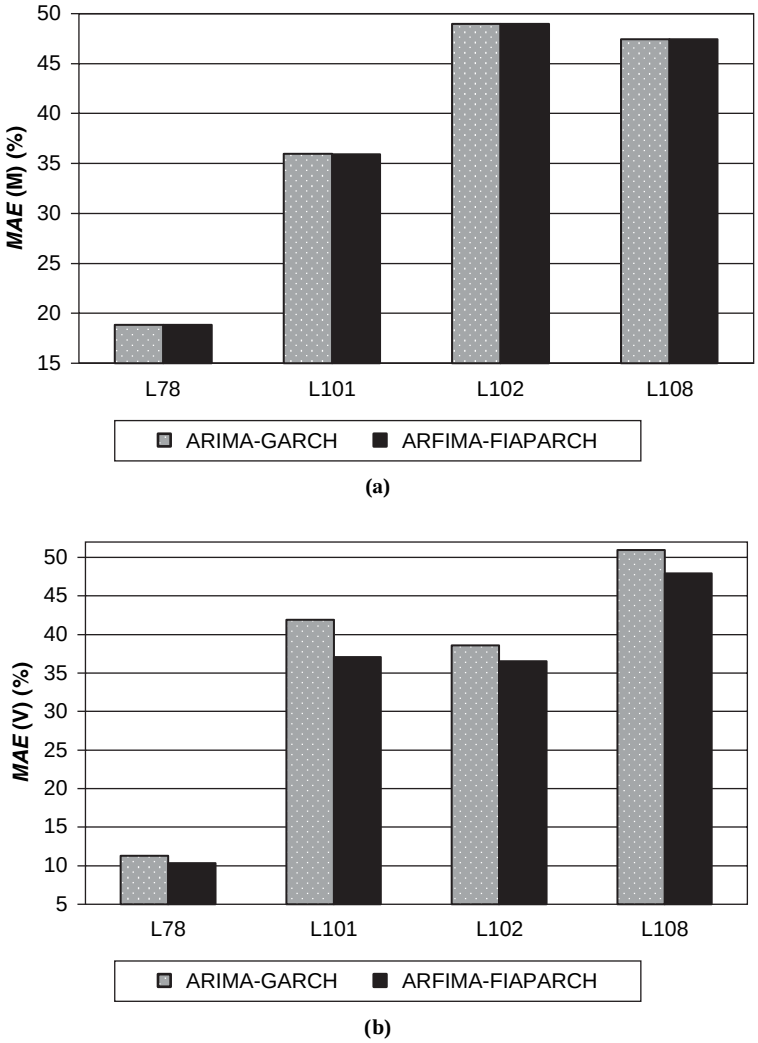


FIGURE 4 Comparison of forecasting performance of ARIMA-GARCH and ARFIMA-FIAPARCH models in terms of (*a*) MAE(M) and (*b*) MAE(V) with Prediction Step $h = 5$.

past shocks to decay at a much slower hyperbolic rate over longer lags in comparison with the ARIMA-GARCH model. Besides, the similarity of the volatility forecasts for steps $h = 5$ and $h = 10$ (Figure 2*b* and *c*) in comparison with the forecast corresponding to $h = 1$ (Figure 2*a*) verifies that the effect of shocks fades away at a decreasing rate as time passes. The length of the forecasting horizon beyond which the models are not able to provide any information about the impact of shocks on volatility can vary significantly with the data aggregation frequency and the topological and traffic characteristics of each network setting.

## CONCLUSIONS

The modeling and forecasting of traffic volatility dynamics is a key element in understanding and addressing the uncertainty pertaining to the operation of urban arterial networks. This study investigated the development and the forecasting performance of an autoregressive heteroscedastic model referred to as ARFIMA-FIAPARCH, which incorporates fractionally integrated components in both the conditional mean and the conditional variance equations. The results of the model fitting procedure verified the statistical significance of the fractionally integrated process in the conditional variance that allows the effects of shocks to decay at a slow hyperbolic rate in contrast to the standard GARCH process. Moreover, the power transformation in the variance equation renders the model specification more flexible in the sense of increasing the response of the forecasting mechanism to real-time traffic information, expressed by the ratio between volume and occupancy, fed to the model.

The ARFIMA-FIAPARCH model was found to outperform the ARIMA-GARCH model when it is used to provide short-term traffic volatility forecasts. In particular, the ARFIMA-FIAPARCH model improves the accuracy of predicted volatility, and it predicts traffic flow levels with basically the same accuracy as the forecasts of the ARIMA-GARCH model. The proposed methodology can be used to enhance the reliability of the predicted travel times in urban arterial networks through determination of appropriate confidence bounds. These forecasts can be provided to the users either as pretrip information (e.g., through the Internet) or during their trip through

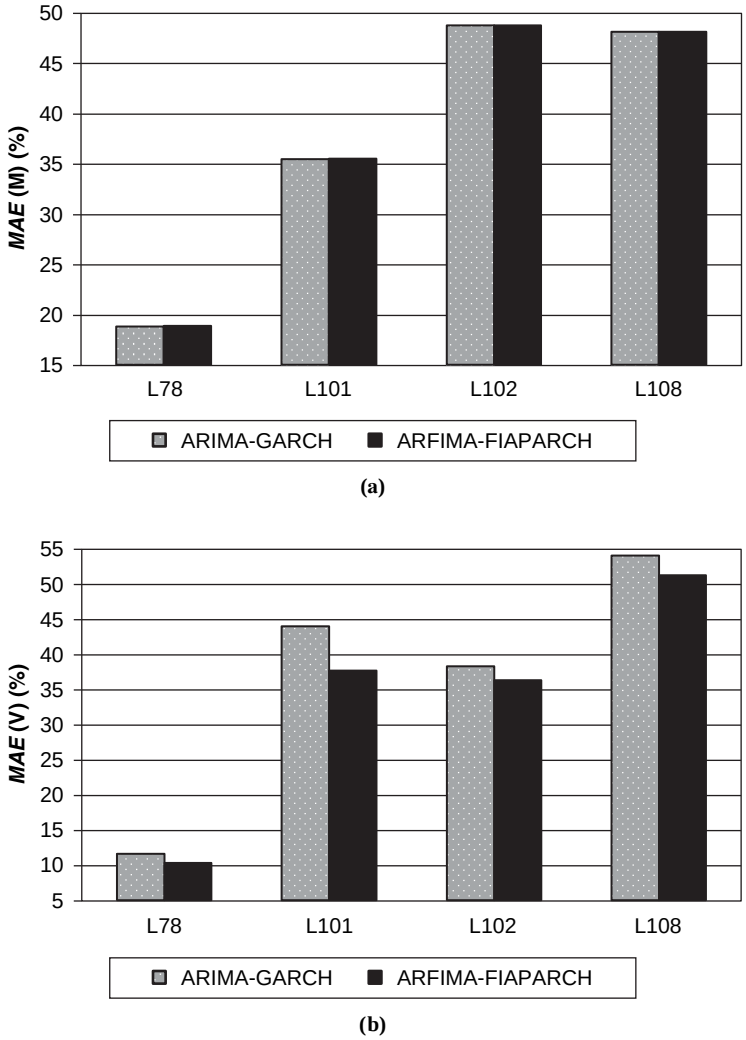


FIGURE 5 Comparison of forecasting performance of ARIMA-GARCH and ARFIMA-FIAPARCH models in terms of (*a*) MAE(M) and (*b*) MAE(V) with Prediction Step $h = 10$.

individual (in-vehicle) or collective (changeable message signs) information systems.

Further work is required to identify and model processes underlying the multiscale temporal and spatial dynamics of traffic volatility in signalized urban networks. These efforts could be directed toward the investigation of the effect of fat tails and multiperiod statistical distributions on volatility predictions over long forecasting periods, such as those of a series of weeks or months, for the most congested arterials and times of day. Further research should also address the application and comparative evaluation of approaches other than those of ARCH-type models, such as stochastic volatility models (*21*), in which the conditional variance is specified to follow some latent stochastic process.

## REFERENCES

1. Williams, B. M. Multivariate Vehicular Traffic Flow Prediction: Evaluation of ARIMAX Modeling. In *Transportation Research Record: Journal of the Transportation Research Board, No. 1776*, TRB, National Research Council, Washington, D.C., 2001, pp. 194–200.
2. Smith, B. L., B. M. Williams, and R. K. Oswald. Comparison of Parametric and Nonparametric Models for Traffic Flow Forecasting. *Transportation Research*, Vol. 10C, No. 4, 2002, pp. 303–321.
3. Doan, D. L., A. Ziliaskopoulos, and H. Mahmassani. On-Line Monitoring System for Real-Time Traffic Management Applications. In *Transportation Research Record: Journal of the Transportation Research Board, No. 1678*, TRB, National Research Council, Washington, D.C., 1999, pp. 142–149.
4. Yang, F., Z. Yin, H. X. Liu, and B. Ran. Online Recursive Algorithm for Short-Term Traffic Prediction. In *Transportation Research Record: Journal of the Transportation Research Board, No. 1879*, Transportation Research Board of the National Academies, Washington, D.C., 2004, pp. 1–8.
5. Smith, B. L., and M. J. Demetsky. Short-Term Traffic Flow Prediction: Neural Network Approach. In *Transportation Research Record 1453*, TRB, National Research Council, Washington, D.C., 1994, pp. 98–104.
6. Stathopoulos, A., and M. G. Karlaftis. A Multivariate State-Space Approach for Urban Traffic Flow Modelling and Prediction. *Transportation Research*, Vol. 11C, No. 2, 2003, pp. 121–135.
7. Frazier, C., and K. M. Kockelman. Chaos Theory and Transportation Systems: Instructive Example. In *Transportation Research Record: Journal of the Transportation Research Board, No. 1897*, Transportation Research Board of the National Academies, Washington, D.C., 2004, pp. 9–17.

8. Kamarianakis, Y., and P. Prastacos. Forecasting Traffic Flow Conditions in an Urban Network: Comparison of Multivariate and Univariate Approaches. In *Transportation Research Record: Journal of the Transportation Research Board, No. 1857*, Transportation Research Board of the National Academies, Washington, D.C., 2003, pp. 74–84.
9. Kamarianakis, Y., A. Kanas, and P. Prastacos. Modeling Traffic Volatility Dynamics in an Urban Network. In *Transportation Research Record: Journal of the Transportation Research Board, No. 1923*, Transportation Research Board of the National Academies, Washington, D.C., 2005, pp. 18–27.
10. Granger, C. W. J., and R. Joyeux. An Introduction to Long-Memory Time Series Models and Fractional Differencing. *Journal of Time Series Analysis*, Vol. 1, No. 1, 1980, pp. 15–29.
11. Engle, R. F. Autoregressive Conditional Heteroscedasticity with Estimates of the Variance of United Kingdom Inflation. *Econometrica*, Vol. 50, No. 4, 1982, pp. 987–1008.
12. Bollerslev, T. Generalized Autoregressive Conditional Heteroscedasticity. *Journal of Econometrics*, Vol. 31, No. 3, 1986, pp. 307–327.
13. Andersen, T. G., T. Bollerslev, P. F. Christoffersen, and F. X. Diebold. Volatility and Correlation Forecasting. In *Handbook of Economic Forecasting* (G. Elliott, C. W. J. Granger, and A. Timmermann, eds.), North Holland, Amsterdam, 2006.
14. Ding, Z., C. W. J. Granger, and R. Engle. A Long Memory Property of Stock Market Returns and a New Model. *Journal of Empirical Finance*, Vol. 1, No. 1, 1993, pp. 83–106.
15. Tse, Y. K. The Conditional Heteroscedasticity of the Yen-Dollar Exchange Rate. *Journal of Applied Econometrics*, Vol. 13, No. 1, 1998, pp. 49–55.
16. Helbing, D., M. Schönhof, and D. Kern. Volatile Decision Dynamics: Experiments, Stochastic Description, Intermittency Control and Traffic Optimization. *New Journal of Physics*, Vol. 4, 2002, pp. 33.1–33.16.
17. Vlahogianni, E. I., M. G. Karlaftis, and J. C. Golias. Short-Term Traffic Flow Analysis: Detecting and Identifying Nonstationarity and Nonlinearity. Presented at 84th Annual Meeting of the Transportation Research Board, Washington, D.C., 2005.
18. Laurent, S., and J.-P. Peters. G@RCH 2.2: An Ox Package for Estimating and Forecasting Various ARCH Models. *Journal of Economic Surveys*, Vol. 16, No. 3, 2002, pp. 447–485.
19. Doornik, J. A. *Object-Oriented Matrix Programming Using Ox*, 3rd ed. Timberlake Consultants Press, London, 2002. http://www.doornik.com.
20. Chung, C.-F. *Estimating the Fractionally Integrated GARCH Model*. Institute of Economics, Academia Sinica, Taipei, Taiwan, 1999. http://gate.sinica.edu.tw/~metrics/Pdf_Papers/Figarch.pdf.
21. Taylor, S. J. Modelling Stochastic Volatility: A Review and Comparative Study. *Mathematical Finance*, Vol. 4, No. 2, 1994, pp. 183–204.

*The Transportation Network Modeling Committee sponsored publication of this paper.*